Improvement of Camera Characterization Process for Different Capturing Geometries Using Saunderson Surface Correction

Farhad Moghareh Abed, Roy S. Berns; Munsell Color Science Laboratory, Chester F. Carlson Center for Imaging Science, Rochester Institute of Technology, Rochester, NY, USA
Kenichiro Masaoka; NHK Science & Technology Research Laboratories, Tokyo, JAPAN

Abstract

The linearization of camera signals and spectral data is a significant step in the color characterization of image capturing systems. Even though output signals from camera detector usually have a reasonable linear relationship with incident spectral radiance, several factors might lead to slight deviations from perfect linearity. Differences in capturing geometries can be a source of non-linearity between these two quantities. In this research, a surface correction equation is introduced to compensate for differences between the camera signals and reflectance measurement with the aim of improving linearity. We utilized the Saunderson surface correction to account for boundary reflections based on measurement geometries. To investigate the idea, three experimental phases were set up. In the first experiment, the reflectance data from two different spectrophotometers were compared with those from a spectroradiometer in two dissimilar lighting conditions. According to the results, the Saunderson equation is capable of improving the measured reflectances from spectrophotometers to be fit to the actual spectral radiances from the spectroradiometer independent of capturing and lighting geometry. In the second phase of the experiment, a digital still camera was characterized using the measured and surface-corrected spectral reflectances. Finally, in the third phase of the experiment, a ColorChecker SG was imaged and used as independent verification data. According to the results, the surface correction improved the linear correlation of spectral reflectances and camera signals for all geometries and spectral data.

Introduction

In digital photography, one determinant of color quality is the quality of the profile in transforming between device-dependent signals and device-independent colorimetry, either CIEXYZ or CIELAB. The vast majority of profiles use a set of target-based training data where the colorimetric data are based on spectral or colorimetric measurements using standard geometries, most often bidirectional, as specified by the ICC [1, 2]. Several factors must be considered in designing a color target such as material, gamut, the number of color patches, and their distribution within the gamut. The material aspects are particularly important where, ideally, the surface and spectral properties of the target samples are identical to the object being imaged. This research is concerned with the surface properties. The issue is the differences in geometry between the spectrophotometer used to define the target's colorimetry and the camera-taking geometry. The more divergent these geometries and differences in surface properties between the profiling target and object, the greater the colorimetric error.

These errors can be predicted, and in turn reduced, by knowing the precise geometries of the spectrophotometer and imaging system and the bidirectional reflectance distribution function (BRDF) of the color patches comprising the color target. BRDF provides the spectral reflectances of the patches for all possible measurement geometries [3]. Practically, there are two limitations. First, it is very difficult to define the camera-taking geometry with high precision. Second, most targets have unknown BRDF. Thus, this fundamental approach, though attractive, is unlikely to receive adoption. The approach used in this research is common to colorant formulation where it is necessary to account for spectrophotometer geometry in order to transform measured spectral reflectance factor to internal reflectance. Internal reflectance is used to predict colorant mixtures. This is known as the "Saunderson correction," and is used routinely to formulate paints and plastics [4,5]. We will use the Saunderson equations to transform the spectrophotometer spectral data to data that would have resulted if the camera-taking geometry had been used when defining the colorimetry of the target.

Theory

The Saunderson correction considers the internal and external reflections that occur due to changes in refractive index at the surface of a paint layer. The equation corrects the *measured reflectance, R_m,* for surface reflections. The corrected reflectance is called *internal reflectance, R_i,* which describes the true amount of diffuse light inside the paint layer. The original equation was derived by Ryde for the general form of incident light and translucent materials [4]. He also simplified the equation for two diffuse and parallel incident lights for a translucent plastic layer. Later, Saunderson applied the Ryde correction equation for color formulation of opaque pigmented plastics using Kubelka-Munk theory. The correction equation is known after Saunderson's name according to applicability of the simplified equation in industry, shown in Eq.1 for 0:d geometry [5]:

$$R_m = \frac{(1-k_1)(1-k_2)R_i}{1-k_2 R_i} + \frac{k_1}{2} \quad (1)$$

where k_1 and k_2 are the proportion of reflected light at the surface. k_1 refers to reflected light at the external surface of the paint and k_2 is the reflected light at the surface internally. These coefficients have been already calculated and optimized for specific measurement geometries, materials and incident light angles according to available spectrophotometer geometries [4-6]. k_1 is specified using the Fresnel equation as a function of incident angle and refractive index of the surface whereas k_2 is usually determined experimentally because most materials are not perfectly diffuse [4]. Dividing k_1 by 2 in Eq. 1 is due to the loss of specular

reflectance through the entrance hole of the integrating sphere [5]. Similarly, the Saunderson equation is defined slightly different in different references to account for different measurement geometries. For d:0 geometry with specular component included (SPIN), the Saunderson correction equation is recommended to be as Eq. 2 since all the surface reflectances reach the detector [7-11].

$$R_m = \frac{(1 - k_1)(1 - k_2)R_i}{1 - k_2 R_i} + k_1 \qquad (2)$$

With the same explanation, it is recommended to remove the separate k_1 term from the Eq. 2 for specular excluded (SPEX) and bidirectional geometries [8]. In a more comprehensive form of the equation, another coefficient, k_{ins}, is added to describe the geometry of the measurement as shown in Eq. 3 [12].

$$R_m = \frac{(1 - k_1)(1 - k_2)R_i}{1 - k_2 R_i} + k_{ins}k_1 \qquad (3)$$

k_{ins} describes the proportion of external reflected light received by the detector as a factor of measurement geometry. k_{ins} is set to 1 for total reflectance or SPIN geometry and 0 for 45:0 and SPEX geometries [7, 12]. However specifying these predefined values for k_{ins} even for a given spectrophotometer with known geometry is not accurate. It is also important to note that k_1 and k_2 also depend on the incident light angle and must be changed according to the measurement geometry [4, 6]. Because of these reasons, Saunderson coefficients usually are optimized in an iteration loop to improve the linearity and scalability in prediction models [8].

When we consider a camera as a measurement device, the Saunderson equation can be used in the same manner. This correction can account for the difference between the spectral radiance reaching the camera detector and the spectrophotometer. In this research we optimized the Saunderson coefficients for the changes in spectral measurement and image capturing geometry. The process of reflectance correction is shown in Figure 1. In this figure, the measured spectral reflectance from the spectrophotometer, R_m, is converted to the internal reflectance, R_i, using Eq. 1 and according to the geometry of the spectrophotometer. Afterward, internal reflectance is converted to total reflectance factor, $R_{m,c}$, based on the geometry of the camera system.
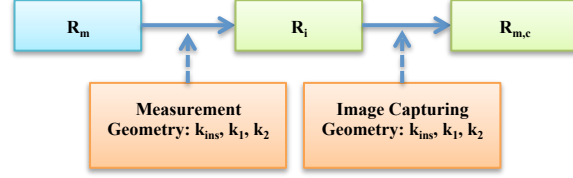

Figure 1. The workflow of correcting the measured reflectance for different geometries.

The Saunderson coefficients are not known for the image capturing system since its geometry is not defined precisely; thus those coefficients are optimized to have the maximum linearity with the linearized capturing signals. The linearity between input (entrance radiance) and output signals (camera signals) improves the characterization process because RGB data are assumed to have a linear relationship with incoming radiance to the camera [13]. The optimization process is illustrated in Figure 2. In this flowchart, the measured reflectance data R_m of the color target are converted to internal reflectance R_i using Saunderson coefficients according to Eq. 1 (step 1). Then, the calculated internal reflectance is converted back to reflectance factor $R_{m,c}$ but based on the new Saunderson coefficients and Eq. 2 (step 2). Next, CIEXYZ values of the patches are calculated based on corrected reflectances (step 3). Afterward, the camera system is characterized using the calculated CIEXYZ values and camera signals using a simple (3 x 3) matrix (step 4). The estimated CIEXYZ values are compared to the calculated CIEXYZ values by calculating ΔE_{xyz} (step 5). We used ΔE_{xyz} because the tristimulus values have a linear relationship with the spectral data and for the camera, only colorimetric data were estimated. The choice of white point and observer does not affect linearity severely; therefore standard illuminant D65 and the 1931 standard observer were used due to easiness in calculating perceptual color difference in the next steps. The optimization algorithm optimized the Saunderson coefficients to minimize ΔE_{xyz} (step 6). The optimization loop uses initial values of Saunderson coefficients based on proposed coefficients in the literature [5-7]. Finally, the optimized Saunderson coefficients are used for calculating corrected reflectances used for camera characterization. It is important to note that this process can be included into common camera profiling since it does need any further information or measurements compared to regular characterization methods.
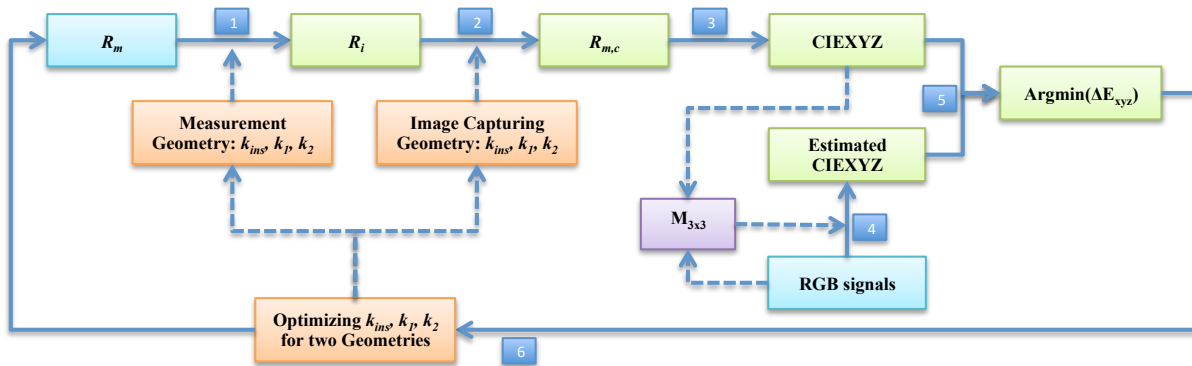

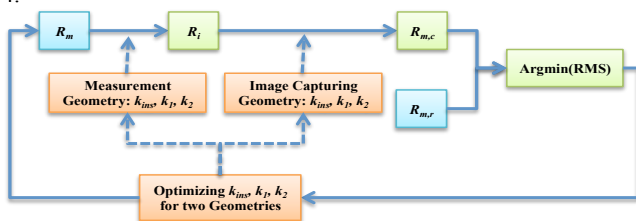*Figure 2*. The workflow of optimizing Saunderson coefficients for camera profiling.

Figure 3. *Lighting and capturing setups for measuring the spectral radiance by PR655. Left: incandescent lighting geometry. Right: diffuse lighting geometry.*

Figure 5 *Lighting and capturing setups using digital camera. Left: incandescent lighting geometry. Right: diffuse lighting geometry.*

Experimental

The Xrite ColorChecker Classic with 24 color patches was used to build profiles. The reflectance data were measured using the Xrite Eye-one with 45°a:0° geometry and the ColorEye 7000 with di:8° (SPIN and SPEX) geometry. The color target was imaged and evaluated in three phases. In the first phase, the general idea of using the Saunderson equation was evaluated. Hence, a Photo Research PR-655 SpectroScan tele-spectroradiometer was used for measuring spectral radiance instead of a digital camera to eliminate any possibilities of non-linearity caused by the camera system (e.g., sensor non-linearity, optical flare, fall-off, etc). Therefore, any differences between reflectances are due to the geometric dissimilarities. 14 gray patches with glossy and matte surfaces were made and the spectral radiances were measured. The gray patches were chosen because they are insensitive to errors in wavelength misalignments and bandwidth differences between the spectrophotometers and spectroradiometer. The spectral reflectance of each sample was obtained using pressed Polytetrafluoroethylene (PTFE) as a reference white. PTFE has a reflectance factor of almost one in all visible wavelengths and has a surface property close to a Lambertian surface. The measurements were done for two different lighting and capturing geometries as shown in Figure 3.

In order to have a constant lighting and capturing geometry, the position of the PR655 was kept fixed while each sample was positioned at the optical axis sequentially. In the first geometry, the target was imaged under a GTI EVS light booth with rather diffuse fluorescent simulated D50 lighting. In the second geometry a common incandescent light bulb was used for illumination (Figure 3). For this phase of the experiment, the Saunderson coefficients were estimated based on minimizing the RMS values between spectroradiometer and spectrophotometers as illustrated in Figure 4.

Figure 4. *The workflow of optimizing Saunderson coefficients by minimizing spectral RMS values.*

In the second phase, the effect of the algorithm was evaluated for characterizing a digital camera. A Canon Rebel XSi digital SLR camera with EF-S 18-55mm f/3.5-5.6 IS Lens was selected to evaluate the profiling process using the same lighting geometries as the first phase, shown in Figure 5.

The images were captured in raw format with 12 megapixel resolution. The exposure time and aperture size of the camera were adjusted to have no saturated (for bright sample) and no clipped (for dark samples) colors. It was assumed that the camera sensor sensitivity was linear with respect to radiances of the patches. After taking the images, a uniform plate of PTFE field was used to correct the non-uniformity of the lighting system (also known as flat field correction). The RGB values of each patch were averaged after black current correction and used to derive the (3 x 3) transformation matrix. The process was repeated using both the measured and corrected reflectance data.

In the third phase, a ColorChecker SG was imaged and used as independent verification data. The ColorChecker SG has a semi-gloss surface whereas the ColorChecker Classic with matte patches. We only evaluated the 24 color patches of the SG corresponding to the Classic to eliminate errors caused by differences in color gamut.

A non-linear iterative method based on quadratic programming (QP) was used for optimization (*fmincon* command in Matlab). The Saunderson coefficients were constrained to be between zero and unity to have physical meaning. Optimization iteration rapidly converged to the optimum values for all the geometries.

Results and Discussion

The spectral reflectances measured by the two spectrophotometers and the spectroradiometer in phase one of the experiment are compared in Figure 6. Due to surface dissimilarities, the reflectances are not the same for the different measurement geometries as expected. The differences were larger when the incandescent light bulb was used. This geometry, which is almost an anisotropic geometry, is dissimilar to both spectrophotometers having either an integrator sphere or ring geometries.
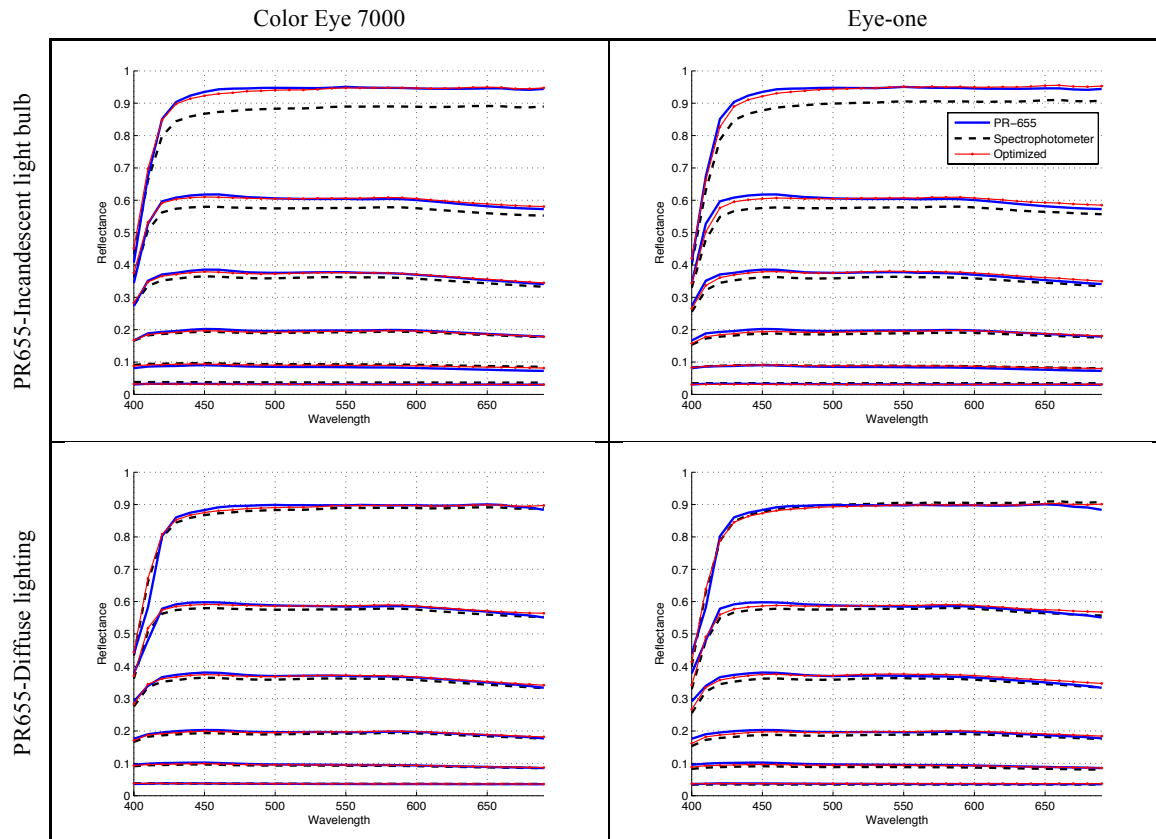
Figure 6. *Corrected and measured spectral reflectances of different spectrophotometers and PR655 in different lighting geometries for six gray patches of The Xrite ColorChecker Classic.*

The optimized coefficients of the four capturing geometries are summarized in Table 1. According to this table, k_{ins} for spectral measurements by spectrophotometers are larger than k_{ins} values of spectral radiance measurements when the light bulb was used. In other words, both of the spectrophotometers detect larger amounts of specular reflectance compared to this geometry. On the other hand, the Saunderson coefficients are about the same for incoming and outgoing light flux in diffuse geometry, which imply almost identical geometry for radiometric and spectrophotometric measurments. However, it is important to note that the optimized coefficients are relative values and do not express absolute physical metrics.

Table 1: Optimized coefficients in different capturing geometries.

		Incandescent		Diffuse	
		EyeOne	ColorEye	EyeOne	ColorEye
Incoming	k_1	0.05	0.07	0.03	0.03
	k_2	0.51	0.58	0.60	0.59
	k_{ins}	0.10	0.10	0.54	0.47
Outgoing	k_1	0	0	0.05	0.03
	k_2	0.50	0.59	0.57	0.58
	k_{ins}	0	0	0.42	0.52

The result of fitting the spectral reflectances using the Saunderson correction is also shown in Figure 6 (red lines). The corrected reflectances have almost the same differences in all geometries in spite of dissimilar geometries. Applying the Saunderson correction decreased the differences between the two sets of reflectances. Note that the optimization process is independent of any information about the geometry of the lighting and spectral measurements. It can be concluded that, the Saunderson correction is capable of eliminating the effect of geometric differences.

In the second phase of the experiment, the digital camera was characterized by the two sets of spectral reflectance data. Color difference values are shown in Figures 7 and 8. The mean and variance of ΔE_{xyz} for both sets of reflectances are compared in Figure 7. The variance is a metric of the amount of noise after the transformation. Both mean and variance of the error are important factors in high quality and precise color reproduction pipelines. The mean and variance of ΔE_{xyz} were decreased after the Saunderson correction in all cases. The Saunderson correction improved the profiling process by compensating for geometrical dissimilarities in all cases.

The perceptual color differences (mean of CIEDE2000) of the traditional and new methods are depicted in Figure 8. For diffuse geometries, the Saunderson correction enhanced the prediction up to 0.5 CIEDE2000. The color differences can be evaluated by looking at CIELAB values of actual and predicted data plotted in

Figure 9. Notice that the correction specifically led to better predictions for dark samples after Saunderson correction. Appearance changes due to measurement geometries are the result of internal and external specular reflectance differences, which usually causes slight luminance changes (for isotropic surfaces). These changes in luminance level are more visible in dark samples. Correcting for linearity improved the characterization process to be valid for dark samples with better accuracy. Considering that the dark samples have small colorimetric coordinates therefore they are less effective in regression algorithms. Hence, if camera signals and spectral measurements are not linearly related, a 3x3 matrix from regular regression method usually leads to better fit for color patches with larger tristimulus values.
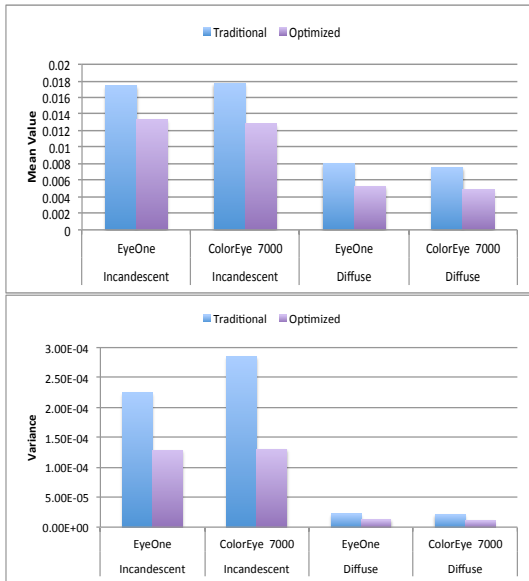
Even though the Saunderson correction improved the accuracy of the predictions, the capturing geometry affects the characterization process more effectively than the spectrophotometer geometry in this research. According to the mean and variance values, the incandescent light bulb with almost 45°a:0° geometry led to larger errors regardless of the spectrophotometer geometry. According to Figure 7, the mean and variance of the error values are larger for incandescent capturing geometry (anisotropic). The larger error can be because of lower luminance level in incandescent geometry. The illuminance level for the incandescent geometry was about 280 Lux compare to 1680 Lux for diffuse geometry. There are other factors such as the spectral sensitivity of the sensors or the deviation of reference white from a Lambertian surface could affect the accuracy of measured, which was beyond the concept in this paper.

Figure 7. Comparison of mean (top) and variance (bottom) value of ΔE$_{xyz}$ for regular and optimized spectral reflectances. The first line in the x-axis specifies the spectrophotometer used for measuring the spectral data. The second line in the x-axis specifies the capturing geometries correspond to Figure 5.
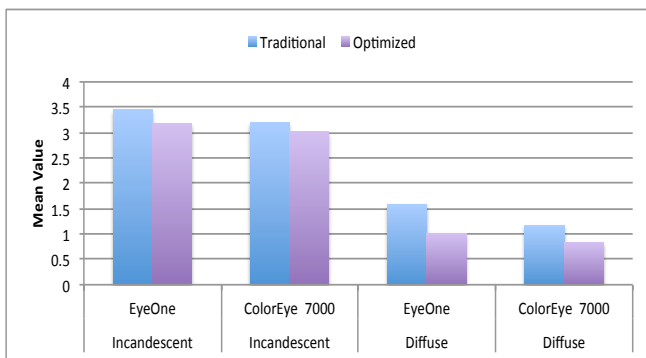

Figure 8. Comparison of mean of DIEDE2000 values for traditional and optimized methods. The first line in the x-axis specifies the spectrophotometer used for measuring the spectral data. The second line in the x-axis specifies the capturing geometries correspond to Figure 5.
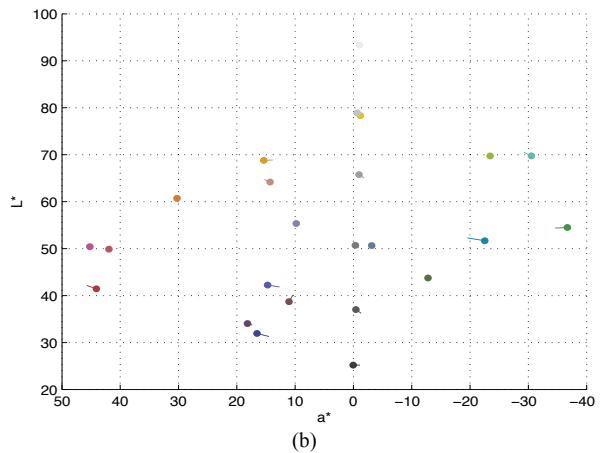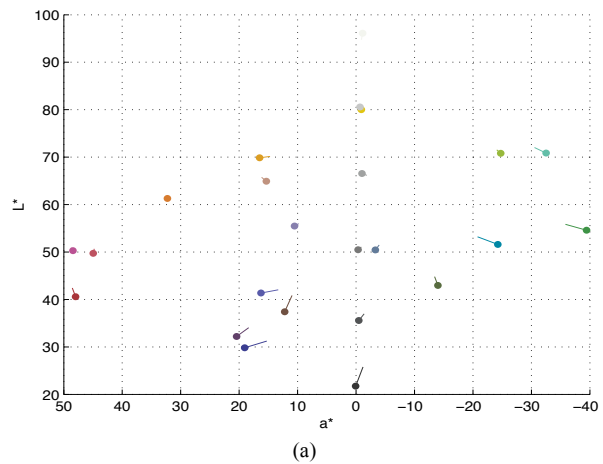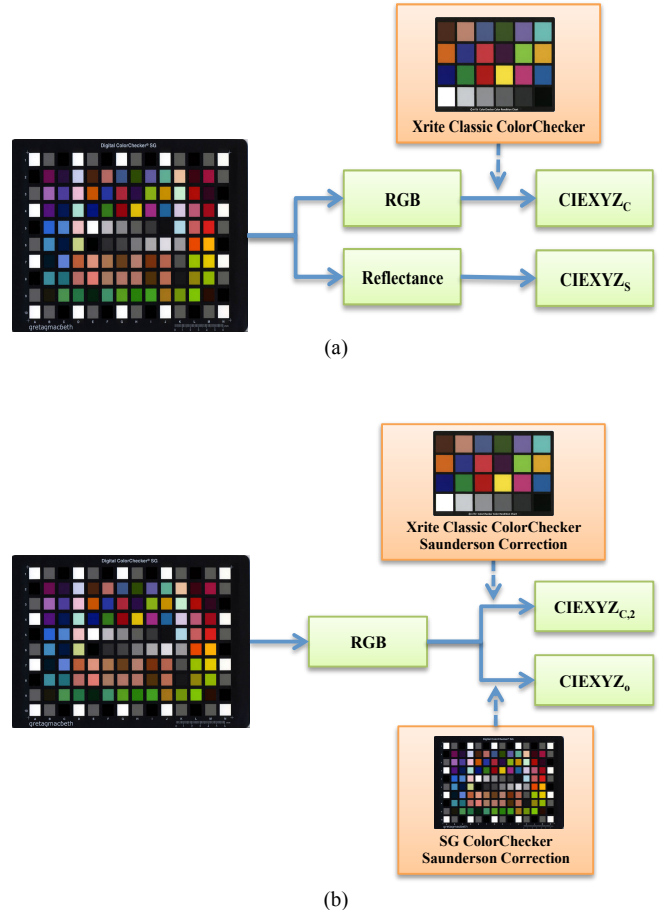

(a)

(b)

Figure 9. Comparison of regular (a) and optimized method using Saunderson correction (b) in CIELAB color space. In each plot filled circles represent actual values of the color checker. The line connected to each circle shows the location of the predicted value. These plots are correspond to diffuse image capturing geometry and spectral measurements by eye one spectrophotometer.
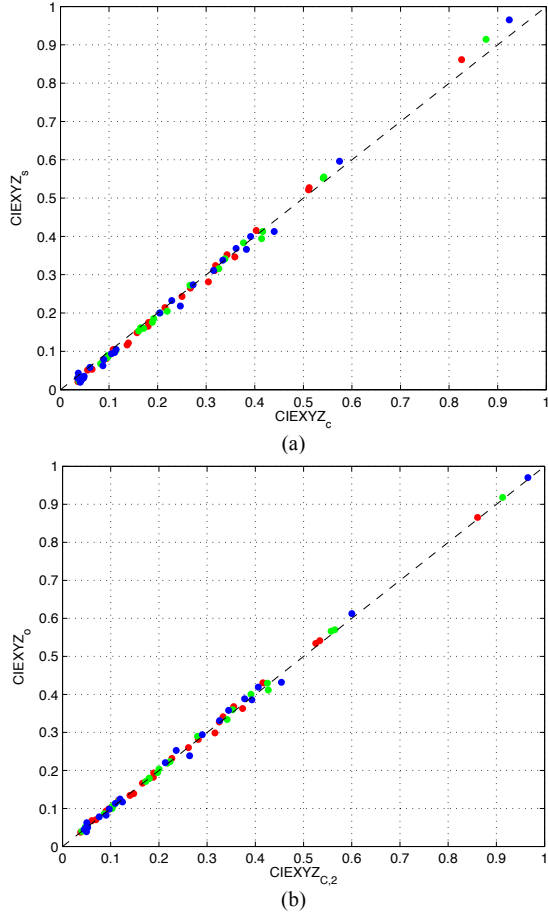
Figure 10. Estimated CIEXYZ values of 24 color patches of SG ColorChecker using two characterization methods for diffuse lighting. Red, Green and blue dots are corresponded to CIE X, Y and Z values.

Figure 11. The workflow of calculating CIEXYZ values in Phase III. (a): regular characterization method using a 3 by 3 matrix, (b): characterization after Saunderson correction.

The results of the CIEXYZ estimation for the third phase are shown in Figure 10. Comparing CIEXYZ from spectrophotometer and camera was not possible because the true spectral radiance of the SG color checker during image capture was unknown. To evaluate the efficiency of new characterization process we designed a workflow shown in Figure 11 (b). The regular profiling workflow that uses only a (3 x 3) matrix for the transformation is also shown in Figure 11 (a). The calculated tristimulus values from the Eye-one spectrophotometer ($CIEXYZ_s$) and the CIEXYZ from camera after characterization using the regular methods ($CIEXYZ_c$), corresponding to Figure 11 (a), is illustrated in Figure 10(a). It shows that a 3x3 transformation matrix cannot correct the estimated tristimulus values from the camera and spectrophotometer with appropriate accuracy particularly for very dark and very light patches. In Figure 10 (b), the estimated CIEXYZ values from phase II ($CIEXYZ_{C,2}$) is plotted against CIEXYZ when the ColorChecker SG was used as the training data ($CIEXYZ_o$). $CIEXYZ_o$ are tristimulus values when Color Checker SG is used for characterization and optimizing the Saunderson coefficients (corresponding to Figure 11(b)). According to Figure 11 (b), XYZ values using both color checkers have a reasonable correlation when Saunderson correction is utilized. It can be concluded that the profiling process has become more independent

of the color checker material and surface characteristics by employing the Saunderson correction.

Conclusions

In this research the Saunderson equation was used for compensating for geometrical dissimilarities between a still camera and two spectrophotometers. The Saunderson coefficients were optimized to obtain the best linearity between camera signals and spectrophotometers in different geometries. Three experimental phases were conducted to evaluate the performance of the colorimetric characterization after surface correction.

In the first phase of the experiment, the influence of the Saunderson correction was assessed by spectroradiometric measurements. The correlation of the radiometric measurement with the spectrophotometric data was evaluated for different geometries. According to the results, the Saunderson correction reflectance can compensate for the changes in measurement geometries to fit to the radiometric spectral reflectances.

In the second phase of the experiment, the Saunderson correction was used in color characterization of a digital camera. The Saunderson correction reduced the ΔE_{xyz} and CIEDE2000 values for target patches, which are important factors in high-quality color reproduction workflows. The Saunderson correction

specifically improved the predictions for dark samples. Also, among different capturing geometries, diffuse geometries had less variations and better correlations with the spectral data from spectrophotometers. Generally, the capturing geometry has more significant influence on the predictions compared to the Saunderson correction.

Finally, in the third phase of the experiment, the Xrite ColorChecker was used for camera characterization to estimate the colorimetric values of color patches of the ColorChecker SG with distinct surface characteristics. The Saunderson correction led to better estimations even though the color patches in the ColorChecker SG have different surface characteristics.

Acknowledgement

References

[1]   Phil Green, Color Management: Understanding and Using ICC Profiles (West Sussex, United Kingdom: Wiley, 2010)

[2]   International Color Consortium (ICC), http://www.color.org.

[3]   Julie. Dorsey, Holly Rushmeier, and François Sillion, Digital modeling of material appearance (Morgan Kaufmann, MA, 2008).

[4]   J. Ryde, The scattering of light by turbid media. Part I, Proc. R. Soc. London Ser. A, pg. 451. (1931).

[5]   J. Saunderson, "Calculation of the color of pigmented plastics," Jour. Optical Socienty of America A, 32, 727 (1942).

[6]   J. Ryde and B. Cooper, The Scattering of light by turbid media. Part II, Proc. R. Soc. London Ser. A, pg. 464. (1931).

[7]   Roderick McDonald, Colour Physics for Industry, 2nd edition, (Society of Dyers and Colourists, England, 1997) pg. 304.

[8]   Roy S. Berns, Billmeyer and Saltzman's principles of color technology 3rd ed. (Wiley, NY, 2000) pg.165.

[9]   Eugene. Allen, Colorant formulation and shading, Optical radiation measurements vol. 2, (Academic Press, NY, 1980) pg. 307.

[10] R. Kuehni, Computer color formulation, (Lexington Book, MA, Lexington Book, 1975) pg. 16.

[11] Georg. A. Klein, Industrial Color Physics (Springer, NY, 2010) pg 336.

[12] Hans. G. Völz, Industrial color testing 2nd ed. (Wiley VCH, Germany, 2001) pg 75.

[13] Raja Bala, Digital color imaging handbook, chapter 5: Device Characterization (CRC Press, NY, 2002).